Sb···Sb and Bi···Bi Interactions in $Cs_8M_4(P_2Se_6)_5$ (M= Sb, Bi)

Timothy J. McCarthy,† Tim Hogan,‡ Carl R. Kannewurf,‡ and Mercouri G. Kanatzidis*,‡,§

Department of Chemistry and Center for Fundamental Materials Research, Michigan State University, East Lansing, Michigan 48824, and Department of Electrical Engineering and Computer Science, Northwestern University, Evanston, Illinois 60208

Received February 15, 1994. Revised Manuscript Received May 11, 1994®

$Cs_8M_4(P_2Se_6)_5$ (M = Sb, Bi) were synthesized by reacting Bi (Sb) with a molten mixture of $Cs_2Se/P_4Se_{10}/Se$ at 460 °C. The structure features weak M···M interactions and a $[P_2Se_6]^{4-}$ ligand in three unique bonding modes. The $[M_4(P_2Se_6)_5]_n^{8n-}$ layers are composed of $[M_4(P_2Se_6)_4]$ zigzag chains that are linked via $[P_2Se_6]^{4-}$ ligands to form a staircase layered framework. The layers are interdigitated to form tunnels along the *b* direction. Cs^+ ions are found in the tunnels and within the layers. The dark red crystals of $Cs_8Sb_4(P_2Se_6)_5$ **(I)** (75% yield) and the black crystals of the isostructural $Cs_8Bi_4(P_2Se_6)_5$ **(II)** (90% yield) are stable in air and water. Compound **I** crystallizes in the monoclinic space group $P2_1/n$ (No. 14) with a = 15.489(3) Å, b = 11.505(2) Å, c = 17.772(3) Å, β = 95.59(2)°, V = 3152 Å^3, Z = 2, and d_c = 4.455g/cm^3, with $F_o^2 > 3\sigma(F\sigma^2)$=3544, number of variables = 236, and $2\theta_{max}$ = 50°. The final R/R_w = 3.2/4.9. Compound **II** is X-ray isomorphous with a = 15.752(4) Å, b = 11.523(2) Å, c = 17.916(2) Å, β = 95.20(2)°, V = 3241 Å^3, Z = 2, and d_c=4.694 g/cm^3, with $F_o^2 > 3\sigma(F\sigma^2)$ = 2598, number of variables = 236, and $2\theta_{max}$ = 50°. The final R/R_w = 5.4/6.7. The optical band gaps of **I** and **II** were determined by optical spectroscopy to be 1.58 and 1.44 eV, respectively. Both compounds melt congruently at 532 (**I**) and 497 °C (**II**).

1. Introduction

Most of the known solid-state selenophosphates contain the ethane-like $[P_2Se_6]^{4-}$ ligand and belong to an important $M_2P_2Q_6$ (Q = S,Se) family of compounds which are structurally related to CdI_2.[1,2] Thus far, transition metals have received the most attention in this system although a few examples with main group elements such as Sn[1c,3] and Pb[1c,4] are known. Sn and Pb are found in trigonal prismatic sites instead of octahedral sites to form a three-dimensional structure type. The acentric $Sn_2P_2S_6$ is a promising ferroelectric material for use in memory devices.[3] It is noteworthy that $In_{1.33}P_2Se_6$ may be suitable for photovoltaic devices[5,6] while other members of the $M_2P_2Q_6$ family have been studied for rechargeable battery[7] and ion-exchange applications.[8] These compounds are typically synthesized by direct combination of the elements in the 500–800 °C temperature range. Recently, several mixed-metal selenophosphates of the $M_2P_2Se_6$ family have been prepared.[9] Other $[P_xSe_y]^{n-}$ units in existence include the rare $[PSe_4]^{3-}$ ligand found in solid-state compounds such as Cu_3PSe_4[10] and Tl_3PSe_4,[11] while the unusual tungsten complex $[W(Se)(PSe_2)(PSe_4)]^{2-}$ contains the unprecedented heteroallylic $[PSe_2]^-$ unit.[12]

Recently, we reported the synthesis of new quaternary metal selenophosphate compounds (KMP_2Se_6; M = Sb, Bi) using molten alkali poly(selenophosphate) fluxes at intermediate temperatures (<600 °C).[13] These $A_x[P_ySe_z]$ fluxes provide excess selenophosphate anions which coordinate to metal centers and perhaps also act as mineralizers. In the unusual layered structure of KMP_2Se_6 we found a $[P_2Se_6]^{4-}$ building block bridging several Bi atoms in a unique bonding mode. The $[P_2Se_6]^{4-}$ ligand chelates to Bi to form corner-sharing octahedra that are linked together in a layered fashion by Se atoms on the $[P_2Se_6]^{4-}$ ligand. To expand this chemistry and explore the generality of this group 15/16 molten salt approach, we investigated the corresponding cesium-containing fluxes. Prior experience in this research leads us to expect

† Michigan State University.
‡ Northwestern University.
§ A. P. Sloan Foundation Fellow 1991–93 and Camille and Henry Dreyfus Teacher Scholar 1993–95.
® Abstract published in *Advance ACS Abstracts*, June 15, 1994.

(1) (a) Klingen, W.; Eulenberger, G.; Hahn, H. *Z. Anorg. Allg. Chem.*, **1973**, *401*, 97–112. (b) Toffoli, P.; Khodadad, P.; Rodier, N. *Acta Crystallogr., Sect. B* **1978**, *34*, 1779–1781. (c) Klingen, W.; Ott, R.; Hahn, H. *Z. Anorg. Allg. Chem.* **1973**, *396*, 271–278. (d) Jandali, M. Z.; Eulenberger, G.; Hahn, H. *Z. Anorg. Allg. Chem.* **1978**, 447, 105–118.

(2) (a) Ouvrard, G.; Brec, R.; Rouxel, J. *Mater. Res. Bull.* **1985**, *20*, 1181–1189. (b) Lee, S.; Colombet, P.; Ouvrard, G.; Brec, R. *Inorg. Chem.* **1988**, *27*, 1291–1294. (c) Lee, S.; Colombet, P.; Ouvrard, G.; Brec, R. *Mater. Res. Bull.* **1986**, *21*, 917–928. (d) Durand, E.; Ouvrard, G.; Evain, M.; Brec, R. *Inorg. Chem.* **1990**, *29*, 4916–4920.

(3) (a) Carpentier, C. D.; Nitsche, R. *Mater. Res. Bull.* **1974**, *9*, 401–410. (b) Carpentier, C. D.; Nitsche, R. *Mater. Res. Bull.* **1974**, *9*, 1097–1100. (c) Arnautova, E.; Sviridov, E.; Rogach, E.; Savchenko, E.; Grekov, A. *Integr. Ferroelectrics* **1992**, *1*, 147–150.

(4) (a) Becker, R.; Brockner, W.; Schäfer, H. *Z. Naturforsch.* **1983**, *38A*, 874-879. (b) Becker, R.; Brockner, W.; Schäfer, H. *Z. Naturforsch.* **1984**, *39A*, 357–361. (c) Yun, H.; Ibers, J. A. *Acta Crystallogr.* **1987**, *C43*, 2002–2004.

(5) (a) Katty, A.; Soled, S.; Wold, A. *Mater. Res. Bull.* **1977**, *12*, 663–666. (b) Diehl, R.; Carpentier, C. D. *Acta Crystallogr., Sect. B* **1978**, *34*, 1097–1105.

(6) Etman, M.; Katty, A.; Levy-Clement, C.; Lemasson, P. *Mater. Res. Bull.* **1982**, *17*, 579–584.

(7) Thompson, A. H.; Whittingham, M. S. U.S. Patent 4,049,879, 1977. (b) Brec, R.; Le Mehaute', A. Fr. Patents 7,704,519, 1977.

(8) (a) Clement R. *J. Chem. Soc., Chem. Commun.* **1980**, 647–648. (b) Michalowicz, A.; Clement R. *Inorg. Chem.* **1982**, *21*, 3872–3877. (c) Joy, P. A.; Vasudevan, S. *J. Am. Chem. Soc.* **1981**, *114*, 7792–7801.

(9) Pfeiff, R.; Kniep, R. *J. Alloys Compounds* **1992**, *186*, 111–133.

(10) Garin, J.; Parthe, E. *Acta Crystallogr.* **1972**, *B28*, 3672–3674.

(11) Fritz, I. J.; Isaacs, T. J.; Gottlieb, M.; Morosin, B. *Solid State Commun.* **1978**, *27*, 535.

(12) O'Neal, S. C.; Pennington, W. T.; Kolis, J. W. *Angew. Chem., Int. Ed. Engl.* **1990**, *29*, 1486–1488.

(13) McCarthy, T. J.; Kanatzidis, M. G. *J. Chem. Soc., Chem. Commun.*, in press.

0897-4756/94/2806-1072$04.50/0

that an increase in alkali cation size could lead to a new structure type based on other $[P_2Se_6]^{4-}$ bonding modes. Indeed, our investigations led to two novel compounds, with remarkably complex structures.

We report here the synthesis, structural characterization, and optical, thermal, and electrical properties of two new isostructural compounds, $Cs_8Sb_4(P_2Se_6)_5$ and $Cs_8Bi_4(P_2Se_6)_5$. Apart from their complicated layered structure, these compounds exhibit a rare example of unusually close Sb···Sb and Bi···Bi interactions, similar in magnitude to those found in the corresponding elements. The ethane-like $[P_2Se_6]^{4-}$ ligand is found in three different and unique bonding modes.

2. Experimental Section

2.1. Reagents. Chemicals in this work were used as obtained: (i) antimony powder, 99.999+% purity, −200 mesh, Cerac Inc., Milwaukee, WI; (ii) bismuth powder, 99.999% purity, −100 + 200 mesh, Johnson Matthey/AESAR Group, Seabrook, NH; (iii) red phosphorus powder, Morton Thiokol, Inc., −100 mesh, Danvers, MA; (iv) selenium powder, 99.5+% purity, −100 mesh, Aldrich Chemical Co., Inc., Milwaukee, WI; (v) cesium metal, analytical reagent, Johnson Matthey/AESAR Group, Seabrook, NH; (vi) DMF, analytical reagent, diethyl ether, ACS anhydrous, EM Science, Inc., Gibbstown, NJ.

2.2. Syntheses. All manipulations were carried out under a dry nitrogen atomosphere in a Vacuum Atmospheres Dri-Lab glovebox. For the preparation of Cs_2Se we used a modified literature procedure.[14]

Cs_2Se. A 5.00-g (38-mmol) aliquot of slightly heated (~30 °C) cesium metal was pipetted into a 250-mL round-bottom flask. A 150-mL volume of liquid ammonia was condensed into the flask at −78 °C (dry ice/acetone bath) under nitrogen to give a dark blue solution. A 1.485-g (19-mmol) sample of Se and a Teflon-coated stir bar were added, and the mixture was stirred for 1 h to give a light blue solution. The NH_3 was removed by evaporation under a flow of nitrogen as the bath slowly warmed to room temperature. The pale orange solid (98% yield) was dried under vacuum overnight, flame-dried, and ground to a fine powder in the glovebox.

P_4Se_{10}. The amorphous phosphorus selenide glass, "P_4Se_{10}", was prepared by heating a stoichiometric ratio of the elements in an evacuated Pyrex tube for 24 h at 460 °C. The glass was ground up and stored in a nitrogen glovebox.

$Cs_8Sb_4(P_2Se_6)_5$ (I). Amounts of 0.018 g (0.15 mmol) of Sb, 0.206 g (0.225 mmol) of P_4Se_{10}, 0.103 g (0.30 mmol) of Cs_2Se, and 0.047 g (0.60 mmol) of Se were thoroughly mixed and transferred to a 6-mL Pyrex tube, which was subsequently flamed-sealed in vacuo (~10^{-3} Torr). The tube was heated to 460 °C over 12 h in a computer-controlled furnace. It was kept at 460 °C for 6 days, followed by cooling to 140 °C at a rate of 4 °C/h and then to room temperature in 1 h. The product, which is stable in water and air, was isolated by dissolving the flux with degassed DMF under inert atmosphere and then washing with anhydrous ether to give 0.120 g (75% yield based on Sb) of pure dark red crystals. Semiquantitative microprobe analysis on single crystals gave $Cs_{2.3}Sb_{1.0}P_{2.3}Se_{7.2}$ (average of three data acquisitions). Far-IR absorbances are given in Table 1.

$Cs_8Bi_4(P_2Se_6)_5$ (II). The reaction of 0.031 g (0.15 mmol) of Bi, 0.206 g (0.225 mmol) of P_4Se_{10}, 0.103 g (0.30 mmol) of Cs_2Se, and 0.047 g (0.60 mmol) of Se under the above conditions gave 0.155 g (90% yield based on Bi) of black crystals. Semiquantitative microprobe analysis on the single crystals gave $Cs_{2.0}Bi_{1.0}P_{1.8}Se_{6.5}$ (average of three data acquisitions.). Far-IR absorbances are given in Table 1.

2.3. Physical Measurements. FT-IR spectra of **I** and **II** were recorded as solids in a CsI matrix. The samples were ground with dry CsI into a fine powder and pressed into transluscent pellets. The spectra were recorded in the far-IR region (600–100 cm^{-1}, 4-cm^{-1} resolution) with the use of a Nicolet 740 FT-IR spectrometer equipped with a TGS/PE detector and silicon beam splitter.

Semiquantitative microprobe analyses of the compounds were performed with a JEOL JSM-35C scanning electron microscope (SEM) equipped with a Tracor Northern energy dispersive spectroscopy (EDS) detector. Data acquisition was performed with an accelerating voltage of 20 kV and a 1-min accumulation time.

Optical diffuse reflectance measurements were made at room temperature with a Shimadzu UV-3101PC double-beam, double-monochromator spectrophotometer operating in the 200–2500-nm region. The instrument was equipped with an integrating sphere and controlled by a personal computer. The measurement of diffuse reflectivity can be used to obtain values for the band gap which agree rather well with values obtained by absorption measurements from single crystals of the same material. The digitized spectra were processed using the Kaleidagraph software program. $BaSO_4$ powder was used as reference (100% reflectance). The data were processed as described earlier.[15]

Table 1. Far-IR Data for $Cs_8Sb_4(P_2Se_6)_5$ (I) and $Cs_8Bi_4(P_2Se_6)_5$ (II)[a]

I	II
522 (m)	518 (m)
511 (m)	499 (s, br)
500 (m)	460 (m, br)
474 (m)	424 (w)
462 (m)	416 (m)
448 (w)	406 (m)
414 (m)	392 (m)
406 (s)	366 (w sh)
394 (s)	337 (vw)
297 (m)	293 (m sh)
287 (s)	289 (m)
204 (m)	280 (m sh)
188 (w)	253 (w sh)
177 (m)	249 (w sh)
149 (s)	226 (w)
	221 (w sh)
	201 (vw)
	192 (m)
	171 (m)
	144 (m)

[a] Abbreviations: s = strong, m = medium, w = weak, sh = shoulder, v = very, br = broad.

Table 2. Crystallographic Data for $Cs_8Sb_4(P_2Se_6)_5$ and $Cs_8Bi_4(P_2Se_6)_5$

	I	II
formula	$Cs_8Sb_4(P_2Se_6)_5$	$Cs_8Bi_4(P_2Se_6)_5$
FW	4228.8	4577.7
a, Å	15.489(3)	15.752(4)
b, Å	11.505(2)	11.523(2)
c, Å	17.772(3)	17.916(2)
α, deg	90.000	90.000
β, deg	95.59(2)	95.20(2)
γ, deg	90.000	90.000
Z; V, Å^3	2; 3152	2; 3241
λ	0.71073	0.71073
space group	$P2_1/n$ (No. 14)	$P2_1/n$ (No. 14)
D_{calc}, g/cm^3	4.455	4.694
μ, cm^{-1}	236.55 (Mo Kα)	321.67 (Mo Kα)
$2\theta_{max}$, deg	50 (Mo Kα)	50 (Mo Kα)
temp °C	−80	23
final R/R_w,[a] %	3.2/4.9	5.4/6.7
total data measured	6100	6261
total unique data	5891	6028
data $F_o^2 > 3\sigma(F\sigma^2)$	3544	2598
no. of variables	236	236
crystal dimensions, nm	0.10 × 0.20 × 0.40	0.08 × 0.10 × 0.15

[a] $R = \sum(|F_o| - |F_c|)/\sum|F_o|$; $R_w = \{\sum w(|F_o| - |F_c|)^2/\sum w|F_o|^2\}^{1/2}$.

(14) Feher, F. *Handbuch der Praparativen Anorganischen Chemie*; Brauer, G., Ed.; Ferdinand Enke: Stuttgart, Germany, 1954; pp 280–281.

(15) McCarthy, T. J.; Ngeyi, S.-P.; Liao, J.-H.; DeGroot, D.; Hogan, T.; Kannewurf, C. R.; Kanatzidis, M. G. *Chem. Mater.* **1993**, *5*, 331–340.

Table 3. Fractional Atomic Coordinates and B_{eq} Values for $Cs_8Sb_4(P_2Se_6)_5$ with Estimated Standard Deviations in Parentheses

atom	x	y	z	B_{eq}
Cs(1)	0.4041(1)	0.2492(2)	0.2902(1)	1.54(7)
Cs(2)	0.0910(1)	0.2202(1)	0.2101(1)	1.20(6)
Cs(3)	0.6898(1)	0.2361(1)	0.4081(1)	1.12(6)
Cs(4)	0.9859(1)	0.2475(1)	0.5015(1)	1.23(6)
Sb(1)	0.7848(1)	0.1302(1)	0.15902(8)	0.59(6)
Sb(2)	0.8176(1)	0.3399(1)	0.02670(8)	0.75(6)
Se(1)	0.8796(2)	0.2477(2)	0.2941(1)	0.9(1)
Se(2)	0.7798(2)	0.2365(2)	0.6027(1)	1.0(1)
Se(3)	0.6700(1)	0.0065(2)	0.0655(1)	0.8(1)
Se(4)	0.7796(1)	-0.0265(2)	0.2676(1)	0.8(1)
Se(5)	0.8790(1)	0.5053(2)	-0.0537(1)	0.9(1)
Se(6)	0.6707(1)	0.4752(2)	0.0412(1)	0.76(9)
Se(7)	0.4881(2)	0.2660(2)	0.5043(2)	1.0(1)
Se(8)	0.6179(2)	0.2145(2)	0.1974(1)	0.9(1)
Se(9)	0.5714(1)	-0.0364(2)	0.3475(1)	1.0(1)
Se(10)	0.2645(2)	-0.0173(2)	0.2578(1)	1.2(1)
Se(11)	1.2075(2)	0.2327(2)	0.4060(2)	1.1(1)
Se(12)	1.0322(1)	0.0122(2)	0.3613(1)	1.1(1)
Se(13)	0.5661(1)	0.5026(2)	0.3666(1)	0.8(1)
Se(14)	0.3297(1)	0.4880(2)	0.4408(1)	1.2(1)
Se(15)	1.0502(1)	0.4977(2)	0.3695(1)	1.4(1)
P(1)	1.1547(4)	0.0536(5)	0.4170(3)	0.8(2)
P(2)	0.5823(3)	0.0399(5)	0.1556(3)	0.5(2)
P(3)	0.4423(3)	0.4463(5)	0.5136(3)	0.4(2)
P(4)	0.6380(4)	-0.0775(5)	0.2488(3)	0.5(2)
P(5)	0.2450(3)	0.4385(5)	0.1269(3)	0.6(2)

[a] B values for anisotropically refined atoms are given in the form of the isotropic equivalent displacement parameters defined as $B_{eq} = (4/3)[a^2B(1,1) + b^2B(2,2) + c^2B(3,3) + ab(\cos\gamma)B(1,2) + ac(\cos\beta)B(1,3) + bc(\cos\alpha)B(2,3)$.

Table 4. Fractional Atomic Coordinates and B_{eq} Values for $Cs_8Bi_4(P_2Se_6)_5$ with Estimated Standard Deviations in Parentheses

atom	x	y	z	B_{eq}
Cs(1)	0.4040(2)	0.2431(3)	0.2888(2)	3.2(1)
Cs(2)	0.0916(2)	0.2203(3)	0.2102(2)	2.8(1)
Cs(3)	0.6903(2)	0.2363(3)	0.4086(2)	2.7(1)
Cs(4)	0.9861(2)	0.2478(3)	0.5019(2)	2.7(1)
Bi(1)	0.7869(1)	0.1275(1)	0.16063(8)	1.94(6)
Bi(2)	0.8180(1)	0.3368(2)	0.0215(1)	2.49(7)
Se(1)	0.8808(3)	0.2458(4)	0.2945(2)	2.1(2)
Se(2)	0.7796(3)	0.2393(4)	0.6031(2)	2.4(2)
Se(3)	0.6654(3)	0.0033(4)	0.0650(2)	2.1(2)
Se(4)	0.7768(2)	-0.0336(4)	0.2697(2)	2.0(2)
Se(5)	0.8763(3)	0.5093(4)	-0.0605(2)	2.4(2)
Se(6)	0.6694(3)	0.4765(4)	0.0393(2)	2.1(2)
Se(7)	0.4936(3)	0.2662(4)	0.5090(3)	2.4(2)
Se(8)	0.6171(3)	0.2128(4)	0.1974(2)	1.9(2)
Se(9)	0.5726(3)	-0.0395(4)	0.3472(2)	2.6(2)
Se(10)	0.2590(3)	-0.0216(4)	0.2558(2)	2.6(2)
Se(11)	1.2010(3)	0.2304(4)	0.4013(3)	2.5(2)
Se(12)	1.0328(3)	0.0072(4)	0.3610(2)	2.5(2)
Se(13)	0.5595(3)	0.5008(4)	0.3647(2)	2.2(2)
Se(14)	0.3311(3)	0.4777(4)	0.4477(2)	2.9(2)
Se(15)	1.0481(3)	0.4970(4)	0.3649(3)	2.8(2)
P(1)	1.1543(6)	0.0501(9)	0.4161(5)	1.6(4)
P(2)	0.5831(6)	0.038(1)	0.1566(5)	1.7(4)
P(3)	0.4467(6)	0.4451(8)	0.5174(5)	1.4(4)
P(4)	0.6379(6)	-0.0789(8)	0.2491(5)	1.3(4)
P(5)	0.2475(6)	0.4363(9)	0.1292(5)	1.6(4)

[a] B values for anisotropically refined atoms are given in the form of the isotropic equivalent displacement parameters defined as $B_{eq} = (4/3)[a^2B(1,1) + b^2B(2,2) + c^2B(3,3) + ab(\cos\gamma)B(1,2) + ac(\cos\beta)B(1,3) + bc(\cos\alpha)B(2,3)$.

Differential thermal analysis (DTA) was performed with a computer-controlled Shimadzu DTA-50 thermal analyzer. The ground single crystals (~15.0 mg total mass) were sealed in quartz ampules under vacuum. An empty quartz ampule of equal mass was sealed and placed on the reference side of the detector. The samples were heated to 600 °C at 10 °C/min and then isothermed for 10 min followed by cooling at 10 °C/min to 100 °C and finally by rapid cooling to room temperature. The reported DTA temperatures are peak temperatures. The DTA samples were examined by powder X-ray diffraction after the experiments.

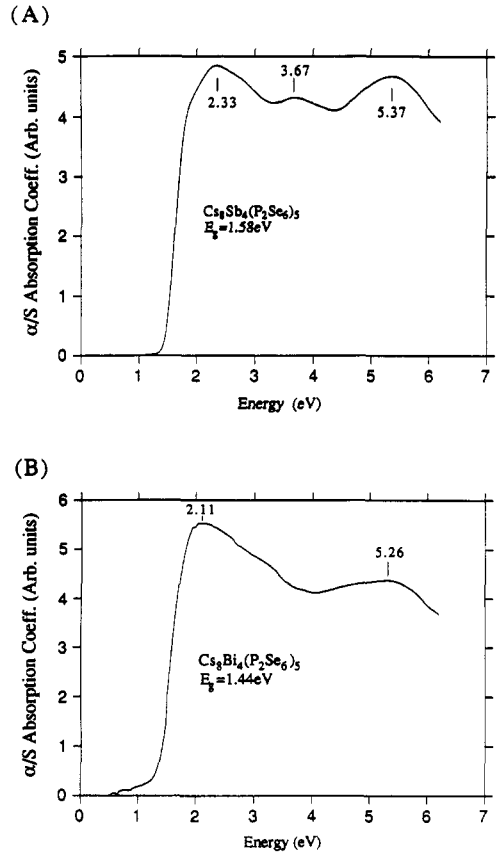

Figure 1. Optical absorption spectra of (A) $Cs_8Sb_4(P_2Se_6)_5$ and (B) $Cs_8Bi_4(P_2Se_6)_5$.

2.4. Charge-Transport Measurements. Direct current electrical conductivity was made on single crystals. Conductivity measurements were performed in the usual four-probe geometry with 60- and 25-μm gold wires used for the current-voltage electrodes. The sample had a very high resistivity so data were obtained above 250 K. Conductivity data were obtained with the computer-automated system described elsewhere.[16]

2.5. Crystallographic Studies. Both compounds were examined by X-ray powder diffraction (XRD) for the purpose of phase purity and identification. Accurate d_{hkl} spacings (angstroms) were obtained from the powder patterns recorded on a Rigaku rotating anode (Cu Kα) X-ray powder diffractometer, Rigaku-Denki/RW400F2 (Rotaflex), at 45 kV and 100 mA with a 1°/min scan rate.

Single-crystal X-ray diffraction data for $Cs_8Sb_4(P_2Se_6)_5$ were collected with a Nicolet P3 four-circle automated diffractometer equipped with a graphite-crystal monochromator. The data were collected with θ–2θ step scan technique. Intensity data for $Cs_8Bi_4(P_2Se_6)_5$ were collected with a Rigaku AFC6 diffractometer equipped with a graphite-crystal monochromator. The data were collected with the $\omega/2\theta$ scan technique. Neither crystal showed any significant intensity decay as judged by three check reflections measured every 150 reflections throughout the data collection. The space groups were determined from systematic absences and intensity statistics. The structures were solved by direct methods of SHELXS-86[17] and refined by full-matrix least-squares techniques of the TEXSAN package of crystallographic programs.[18] An empirical absorption correction based on ψ scans

(16) Lyding, J. W.; Marcy, H. O.; Marks, T. J.; Kannewurf, C. R. *IEEE Trans. Instrum. Meas.* **1988**, *37*, 76–80.
(17) Sheldrick, G. M. In *Crystallographic Computing 3*; Sheldrick, G. M., Kruger, C., Doddard, R., Eds.; Oxford University Press: Oxford, 1985; pp 175–189.
(18) TEXSAN: Single Crystal Structure Analysis Software, Version 5.0, (1981). Molecular Structure Corportion, The Woodlands, TX 77381.

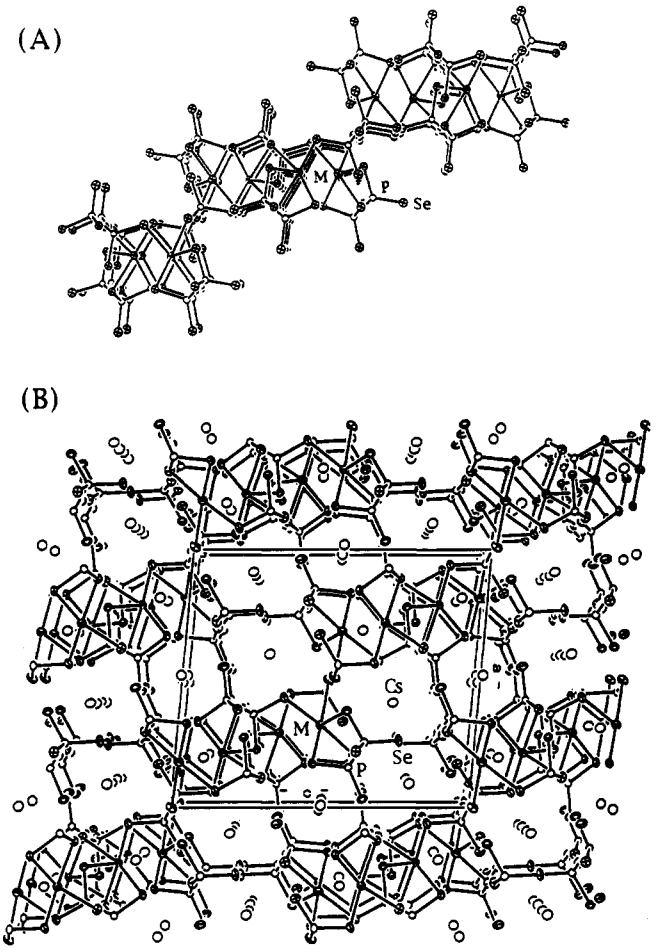

Figure 2. (A) An isolated layer in of $Cs_8Bi_4(P_2Se_6)_5$. (B) Packing diagram of $Cs_8Bi_4(P_2Se_6)_5$ viewed down the [010] direction. The open circles represent Cs atoms.

was applied to each data set, followed by a DIFABS[19] correction to the isotropically refined structure. All atoms were eventually refined anisotropically. The remaining maximum peak height in the Fourier difference density map was less than 1.0 $e^-/Å^3$. Occupancy refinement did not reveal the presence of nonstoichiometry in the compounds. All calculations were performed on a VAXstation 3100/76 computer. The complete data collection parameters and details of the structure solution and refinement for both compounds are given in Table 2. The coordinates of all atoms, average temperature factors, and their estimated standard deviations for both compounds are given in Tables 3 and 4.

3. Results and Discussion

3.1. Synthesis, Spectroscopy, and Thermal Analysis. The syntheses of **I** and **II** were a result of a redox reaction in which the metal is oxidized by polyselenide ions in the $Cs_x[P_ySe_z]$ flux to give M^{3+} species. A $M/P_4Se_{10}/Cs_2Se/Se$ ratio of 1/1.5/2/4 was used to obtain pure compounds. In the case of Bi, decrease in the amount of P_4Se_{10} resulted in Bi_2Se_3 under these conditions.

The far-IR spectra of $Cs_8M_4(P_2Se_6)_5$ are characteristically complex and show a large number of absorptions between 522 and 144 cm^{-1} (see Table 1). Since systematic IR spectroscopic data for selenophosphate ligands are lacking, we cannot assign P–P and $-PSe_3$ vibrational frequencies. However, it is tempting to assign the first two or three higher frequency vibrations to modes due primarily to P–P stretching.[20]

The optical properties of **I** and **II**, studied by UV/near-IR reflectance spectroscopy, suggest semiconducting properties by revealing the presence of sharp optical gaps (see Figure 1); see Figure 1. The bandgaps, E_g, are 1.58 and 1.44 eV, respectively. The slight decrease in band gap in going from Sb to Bi suggests that these metals contribute somewhat to the highest energy levels of the valence band, which is most likely dominated by Se-based orbitals. Based on the calculated solar conversion efficiency versus band gap plot,[21] $Cs_8M_4(P_2Se_6)_5$ would fall near the peak of conversion efficiency. Three absorptions at 2.33, 3.67, and 5.37 eV for **I** and two absorptions at 2.11 and 5.26 eV for **II** are readily resolved and are assigned to electronic Se → M charge-transfer transitions.

Differential thermal analysis (DTA) shows that $Cs_8Sb_4(P_2Se_6)_5$ and $Cs_8Bi_4(P_2Se_6)_5$ melt congruently at 532 and 497 °C, respectively, suggesting that large single crystals or microcrystalline thin films can be grown from the melt.

3.2. Description of Structure. $Cs_8M_4(P_2Se_6)_5$ possesses a remarkably complicated layered structure shown in Figure 2. A stereoview is given in Figure 3. The $[M_4(P_2Se_6)_5]_n^{8n-}$ layers are composed of $[M_4(P_2Se_6)_4]$ zigzag chains that are linked by additional $[P_2Se_6]^{4-}$ ligands to form a staircase layered framework. The layers are interdigitated to form tunnels along the b direction. There are two kinds of cesium ions, one that fills the tunnels and another located within the layers.

There are also three types of $[P_2Se_6]^{4-}$ ligands in this structure each possessing unique denticity. Type 1 is a capping ligand that trichelates to the metal while the other three Se atoms are nonbonding (terminal). Type 2 also trichelates to the metal while two of the remaining Se atoms bond to two separate metals and the sixth Se is terminal. Type 3 chelates to four metals, leaving two nonbonding Se atoms. The P–P bond resides on a center of symmetry. For clarity, the connectivities of the $[P_2Se_6]^{4-}$ ligands are illustrated separately in Scheme 1. It is clear that beyond the well-known $M_2P_2Q_6$ class of compounds and the few other examples that already exist, the $[P_2Q_6]^{4-}$ unit presents excellent new possibilities as a building block

Figure 3. A stereoview of $Cs_8Bi_4(P_2Se_6)_5$.

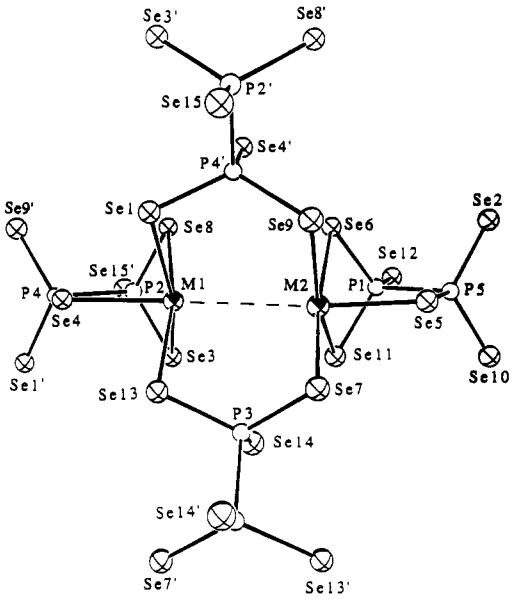

Figure 4. Structure of the $[M_2(P_2Se_6)_4]$ dimeric unit showing the M···M interaction.

Scheme 1

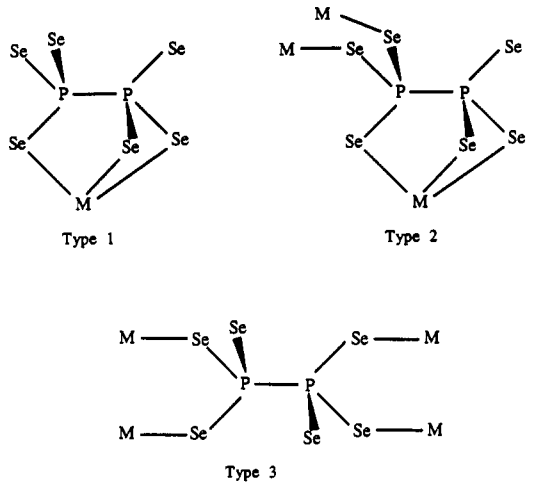

of new frameworks. These possibilities can be readily exploited by the type of molten salt reaction reported here.

One of the most distinguishing features found in this structure are the rather short M···M interactions at 3.534(2) Å for Bi and 3.441(2) Å for Sb (see Figure 4). For comparison, the sum of the van der Waals radii for Bi and Sb is in the range 4.0–4.4 Å. Therefore, the obvious question to ask is, are these significant bonding interactions between these metals or not? To the best of our knowledge, other examples of such remarkably short distances involving these elements are found only in the corresponding elemental structures. Bi metal has an intralayer bond distance of 3.06 Å and an interlayer distance of 3.52 Å. The isostructural Sb metal has distances of 2.90 and 3.34 Å. The longer distances in these metals are considered weakly bonding in nature.[22] We note, however, that the

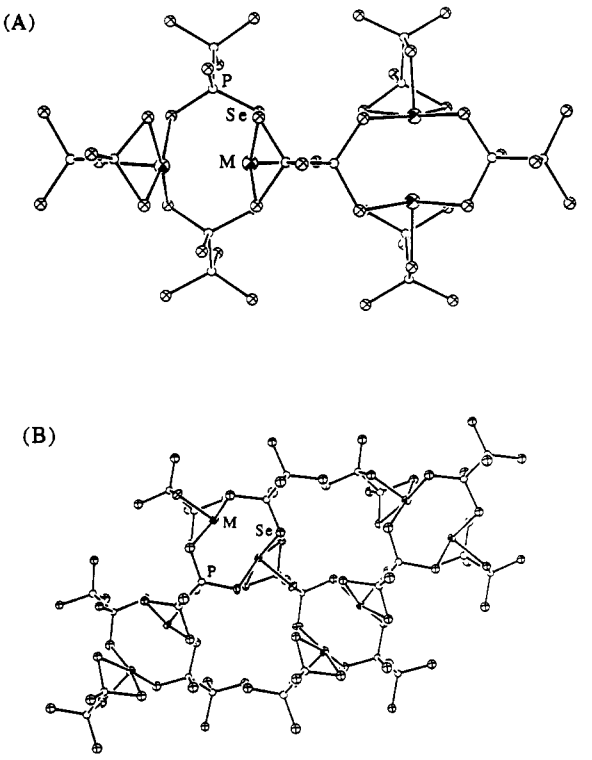

Figure 5. (A) Association of two $[M_2(P_2Se_6)_4]$ "dimers" by a $[P_2Se_6]^{4-}$ unit. (B) Further sharing of $[P_2Se_6]^{4-}$ units among "dimers" results in a one-dimensional chain-like structure.

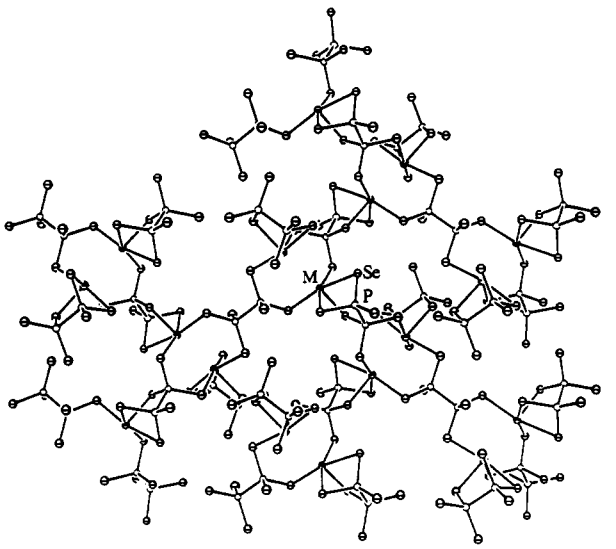

Figure 6. Two-dimensional structure of the $[M_4(P_2Se_6)_5]_n^{8n-}$ anionic framework with labeling as drawn by ORTEP.

metals in the elements are in the zero oxidation state while in **I** and **II** they are in the 3+ state. If a metal–metal bond exists in these compounds, it must form via the interaction of the lone pairs in Sb^{3+} and Bi^{3+}. The $M^{3+}(d^{10}s^2)$ ions with square pyramidal coordination exhibit a stereochemically active lone pair at the base of the pyramid. The bases of the square pyramids in $Cs_8M_4(P_2Se_6)_5$ face each other in close proximity. A weak interaction of this sort is unusual since lone pair/lone pair interactions should be repulsive or nonbonding. Perhaps a closer analog to the case described here is the α,β-PbO where weak Pb···Pb bonding interactions (interlayer Pb···Pb distance of 3.87 Å) were proposed to exist.[23] Closed-shell bonding interactions have also been observed in other systems such as 2,2′,5,5′-tetramethylbistibole $((C_6H_8Sb)_2)$ in which the lone

(19) Walker, N.; Stuart, D. *Acta Crystallogr.* **1983**, *A39*, 158–166.
(20) The characteristic stretching frequency range for P–P interactions of similar interatomic distances is about 400–600 cm^{-1}. Nakamoto, K. In *Infrared and Raman Spectra of Inorganic and Coordination Compounds*; Wiley: New York, 1978.
(21) Loferski, J. J. *J. Appl. Phys.* **1956**, *27*, 777.
(22) (a) Barrett, C. S.; Cucka, P.; Haefner, K. *Acta Crystallogr.* **1963**, *16*, 451–453. (b) Cucka, P.; Barrett, C. S. *Acta Crystallogr.* **1962**, *15*, 865–872.

Table 5. Selected Distances (Å) in $Cs_8M_4(P_2Se_6)_5$ with Standard Deviations in Parentheses[a]

	$Cs_8Sb_4(P_2Se_6)_5$	$Cs_8Bi_4(P_2Se_6)_5$		$Cs_8Sb_4(P_2Se_6)_5$	$Cs_8Bi_4(P_2Se_6)_5$
M–M′	3.441(2)	3.534(2)	Cs(1)–Se (av)	3.9(2)	3.9(1)
M(1)–Se(1)	3.010(3)	3.027(5)	Cs(2)–Se(1)	3.743(3)	3.782(6)
M(1)–Se(3)	2.716(3)	2.838(4)	Cs(2)–Se(2)	3.679(3)	3.700(6)
M(1)–Se(4)	2.648(3)	2.711(4)	Cs(2)–Se(7)	3.849(4)	4.172(5)
M(1)–Se(8)	2.905(3)	2.978(5)	Cs(2)–Se(9)	3.836(3)	3.793(6)
M(1)–Se(13)	2.811(3)	2.898(5)	Cs(2)–Se(10)	3.868(3)	3.864(6)
M(1)–Se (av)	2.8(1)	2.9(1)	Cs(2)–Se(10′)	3.769(3)	3.872(6)
			Cs(2)–Se(11)	3.765(4)	3.807(6)
M(2)–Se(5)	2.613(3)	2.682(5)	Cs(2)–Se(12)	3.775(3)	3.691(6)
M(2)–Se(6)	2.789(3)	2.883(5)	Cs(2)–Se(13)	3.661(3)	3.827(5)
M(2)–Se(7′)	2.970(3)	3.037(5)	Cs(2)–Se(14)	4.059(3)	3.644(5)
M(2)–Se(9′)	3.039(3)	3.132(5)	Cs(2)–Se (av)	3.8(1)	3.8(1)
M(2)–Se(11)	2.739(3)	2.813(5)			
M(2)–Se (av)	2.8(2)	2.9(2)	Cs(3)–Se(1)	3.730(3)	3.783(6)
			Cs(3)–Se(2)	3.600(3)	3.638(5)
P(1)–P(5)	2.240(7)	2.24(1)	Cs(3)–Se(3)	3.797(3)	3.829(6)
P(2)–P(4)	2.244(8)	2.25(1)	Cs(3)–Se(5)	3.928(3)	3.983(5)
P(3)–P(3′)	2.26(1)	2.24(2)	Cs(3)–Se(6)	3.757(3)	3.788(5)
P–P (av)	2.25(1)	2.24(1)	Cs(3)–Se(7)	3.721(3)	3.737(6)
			Cs(3)–Se(8)	3.809(3)	3.863(5)
P(1)–Se(6)	2.222(6)	2.22(1)	Cs(3)–Se(9)	3.738(3)	3.792(6)
P(1)–Se(11)	2.233(6)	2.23(1)	Cs(3)–Se(13)	3.653(3)	3.723(6)
P(1)–Se(12)	2.108(7)	2.13(1)	Cs(3)–Se(14)	4.188(3)	
P(2)–Se(3)	2.230(6)	2.22(1)	Cs(3)–Se (av)	3.8(2)	3.8(1)
P(2)–Se(8)	2.194(6)	2.20(1)			
P(2)–Se(15′)	2.114(6)	2.12(1)	Cs(4)–Se(1)	3.888(3)	3.929(5)
P(3)–Se(7)	2.204(6)	2.20(1)	Cs(4)–Se(2)	3.815(3)	3.866(6)
P(3)–Se(13)	2.225(6)	2.21(1)	Cs(4)–Se(3)	4.098(3)	4.111(5)
P(3)–Se(14)	2.123(6)	2.15(1)	Cs(4)–Se(3′)	3.946(3)	3.908(5)
P(4)–Se(1′)	2.158(6)	2.18(1)	Cs(4)–Se(6)	3.855(3)	3.887(5)
P(4)–Se(4)	2.264(6)	2.25(1)	Cs(4)–Se(6′)	3.991(3)	3.999(5)
P(4)–Se(9′)	2.171(6)	2.16(1)	Cs(4)–Se(8)	3.886(3)	3.928(5)
P(5)–Se(2)	2.139(6)	2.15(1)	Cs(4)–Se(11)	3.978(3)	3.982(6)
P(5)–Se(5)	2.305(6)	2.30(1)	Cs(4)–Se(12)	3.795(3)	3.865(6)
P(5)–Se(10)	2.130(6)	2.13(1)	Cs(4)–Se(12′)	3.884(3)	3.858(5)
P–Se (av)	2.19(6)	2.19(5)	Cs(4)–Se(15)	3.904(3)	3.957(6)
			Cs(4)–Se(15′)	3.795(3)	3.855(5)
Cs(1)–Se(2)	3.687(3)	3.710(6)	Cs(4)–Se (av)	3.90(9)	3.93(8)
Cs(1)–Se(5)	4.077(3)	4.019(6)			
Cs(1)–Se(7)	3.904(4)	4.077(5)			
Cs(1)–Se(8)	3.861(3)	3.883(5)			
Cs(1)–Se(10)	3.763(3)	3.824(6)			
Cs(1)–Se(10′)	3.786(3)	3.769(6)			
Cs(1)–Se(11)	3.842(3)	3.933(6)			
Cs(1)–Se(13)	3.998(3)	4.008(5)			
Cs(1)–Se(14)	4.079(3)	4.162(6)			
Cs(1)–Se(15)	4.161(3)	4.071(6)			

[a] The estimated standard deviations in the mean bond lengths and the mean bond angles are calculated by the equations $\sigma_l = \{\sum_n (l_n - l)^2/n(n-1)\}^{1/2}$, where l_n is the length (or angle) of the nth bond, l the mean length (or angle), and n the number of bonds.

pairs in each Sb interact with other dimers by Sb···Sb interactions (3.625 Å) to form one-dimensional chains.[24] This Sb–Sb bond length alternation is the result of a Peierls distortion as determined from electronic band structure calculations.[25] Tetramethyldistibane exhibits similar behavior with an intermolecular Sb–Sb distance of 3.678(1) Å,[26] while tetrakis(trimethylsily)dibismuthane shows a corresponding Bi–Bi distance of 3.804(3) Å.[27] Although these M···M distances are longer than those observed in **I** and **II**, they are probably similar in origin. It is noteworthy that the case of M···M interaction is unique in **I** and **II** in the sense that they are the only examples where "inert" ns^2 lone pairs face directly at each other. Other closed-shell systems such as the classical d^{10}–d^{10} (Cu^+, Ag^+, Au^+) interactions have also been well documented.[28,29] Extended Hückel calculations have shown that mixing of empty 4s and 4p orbitals with occupied 3d orbitals lowers the energy of the σ and σ^* orbitals for several copper complexes.[30] A similar type of interaction, due to mixing with empty p orbitals, could exist in $Cs_8M_4(P_2Se_6)_5$. It has also been proposed for several d^{10}–d^{10} complexes that the bridging ligands bring the metals closer in order to maximize M–L interactions.[31] Since $Cs_8M_4(P_2Se_6)_5$ features two $[P_2Se_6]^{4-}$ bridging ligands for each dimer,

(23) Trinquier, G.; Hoffmann, R. *J. Phys. Chem.* **1984**, *88*, 6696–6711.
(24) Ashe III, A. J.; Butler, W.; Diephouse, T. R. *J. Am. Chem. Soc.* **1981**, *103*, 207–209.
(25) Hughbanks, T.; Hoffmann, R.; Whangbo M.-H.; Stewart, K. R.; Eisenstein O.; Canadell, E. *J. Am. Chem. Soc.* **1982**, *104*, 3876–3879.
(26) Mundt, O.; Riffel, H.; Becker, G.; Simon, A *Z. Naturforsch.* **1984**, *39b*, 317-322.
(27) Mundt, O.; Becker G.; Rössler, M.; Witthauer, C. *Z Anorg. Allg. Chem.* **1983**, *506*, 42–58.
(28) (a) Dance, I. G. *Polyhedron* **1983**, *2*, 1031–1043. (b) Hollander, F. J.; Coucouvanis, D. *J. Am. Chem. Soc.* **1977**, *99*, 6268–6279. (c) Chadha, R.; Kumar, R.; Tuck, D. G. *J. Chem. Soc., Chem. Commun.* **1986**, 188–189. (d) Coucouvanis, D.; Murphy, C. N.; Kanodia, S K. *Inorg. Chem.* **1980**, *19*, 2993–2998.
(29) (a) Burschka, C.; Bronger, W. *Z. Naturforsch.* **1977**, *32B*, 11–14. (b) Burschka, C. *Z. Naturforsch.* **1979**, *34B*, 675–677. (c) Schils, H.; Bronger, W. *Z Anorg. Allg. Chem.* **1979**, *456*, 187–193. (d) Savelberg, G.; Schäfer, H. *Z. Naturforsch.* **1978**, *33B*, 711–713.
(30) (a) Merz, K. M.; Hoffmann R. *Inorg. Chem.* **1988**, *27*, 2120–2127. (b) Mehrotra, P. K.; Hoffmann, R. *Inorg. Chem.* **1978**, *17*, 2187–2189.
(31) (a) Cotton, F. A.; Feng, X.; Matusz, M.; Poli, R. *J. Am. Chem. Soc.* **1988**, *110*, 7077–7083. (b) Lee, S. W.; Trogler, W. C. *Inorg. Chem.* **1990**, *29*, 1659–1662.

Table 6. Selected Angles (deg) in $Cs_8M_4(P_2Se_6)_5$ with Standard Deviations in Parentheses

	$Cs_8Sb_4(P_2Se_6)_5$	$Cs_8Bi_4(P_2Se_6)_5$
Se(1)-M(1)-Se(4)	76.78(8)	78.1(1)
Se(1)-M(1)-Se(8)	92.21(8)	93.4(1)
Se(1)-M(1)-Se(4)	91.41(8)	90.5(1)
Se(1)-M(1)-Se(4)	97.29(8)	100.3(1)
Se(5)-M(2)-Se(9)	81.48(8)	83.2(1)
Se(5)-M(2)-Se(11)	91.49(9)	91.0(1)
Se(6)-M(2)-Se(9)	94.53(8)	93.4(1)
Se(7)-M(2)-Se(11)	105.29(9)	112.0(1)
M(1)-Se(3)-P(2)	83.1(2)	82.6(3)
M(1)-Se(13)-P(3)	98.2(2)	96.7(3)
M(1)-Se(1)-P(4')	95.8(2)	95.3(3)
M(2)-Se(9)-P(4')	102.3(2)	104.1(3)
M(2)-Se(7)-P(3)	94.5(1)	92.7(3)
M(2)-Se(6)-P(1)	80.7(2)	80.1(3)
Se(6)-P(1)-Se(11)	102.6(3)	103.9(4)
Se(6)-P(1)-Se(12)	116.2(2)	116.1(5)
Se(3)-P(2)-P(4)	102.1(3)	103.2(5)
Se(8)-P(2)-Se(15')	119.2(3)	117.9(5)
Se(13)-P(3)-P(3')	100.4(4)	101.9(6)
Se(7)-P(3)-Se(13)	111.7(3)	111.9(4)
Se(1)-P(4')-Se(9)	115.8(3)	115.3(5)
Se(1)-P(4')-Se(4')	112.4(2)	111.9(5)

it is possible that the multidentate $[P_2Se_6]^{4-}$ coordination is playing an important role. It is not clear whether the interactions contribute significantly in determining the structure or the metals are simply forced to tolerate the short contact due to packing forces.

The rest of the structure is built up as follows. Type 1 ligands cap a metal on each M···M dimeric unit (see Figure 4) while one type 2 ligand connects two dimeric units together (see Figure 5). These larger units are assembled into $[M_4(P_2Se_6)_4]$ zigzag chains by additional type 2 ligands. The zigzag chains are connected by type 3 ligands above and below to form the $[M_4(P_2Se_6)_5]_n^{8n-}$ staircase layers as shown in Figure 6.

Selected distances and angles for $Cs_8M_4(P_2Se_6)_5$ are found in Tables 5 and 6. M(1) and M(2) are found in two similar square pyramidal coordination sites (see Figure 4). The M atoms are slightly displaced from their respective square planes. The bond distances of $Cs_8Sb_4(P_2Se_6)_5$ range from the short axial bond distances of 2.648(3) and 2.613(3) Å to 3.010(3) and 3.039(3) Å for Sb(1) and Sb(2), respectively. These compare well with the square pyramidal Sb-Se distances found in $TlSbSe_2$.[32] The bond distances for the Bi analog range from 2.711(4) and 2.682(5) Å to 3.027(5) and 3.037(5) Å, which compare well with those found in $K_2Bi_8Se_{13}$.[15]

The P–P bonds of the $[P_2Se_6]^{4-}$ ligands are normal at 2.25(1) Å (average). The terminal Se atoms have significantly shorter P–Se distances due to partial double bond character.[33] For example, the terminal P(1)–Se(12) distance is 2.108(7) Å while the metal binding Se(6) and Se(11) atoms have P(1)–Se(6) and P(1)–Se(11) distances of 2.222(6) and 2.233(6) Å, respectively.

In $Cs_8Bi_4(P_2Se_6)_5$, Cs(1,2,4) are located in the tunnels that are created by the interdigitated layers. Cs(1) and Cs(2) are 10-coordinate with average Cs–Se distances of 3.9(1) and 3.8(1) Å, respectively. The coordination environment of Cs(1) resembles a tricapped truncated square prism. Cs(2) possesses a bicapped square prismatic coordination. The 9-coordinate Cs(3) (average 3.8(1) Å) resides within the layers in the center of a monocapped square prism. Cs(4) is found in a 12-coordinate tetracapped square prism with an average Cs(4)–Se distance of 3.93(8) Å. The Cs–Se coordination environments are shown in Figure 7.

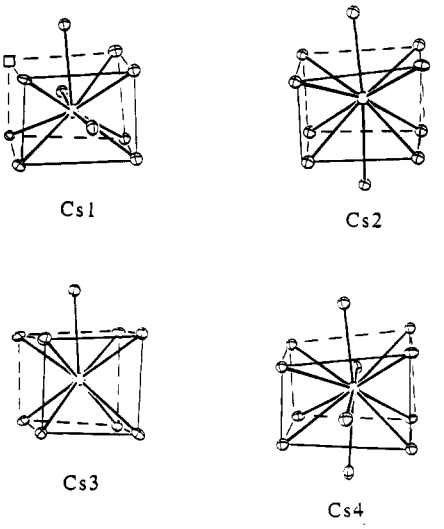

Figure 7. Cs^+ coordination environments. The open circles represent Cs atoms. The open square in the Cs(1) coordination site represents the vacant corner of the square prism.

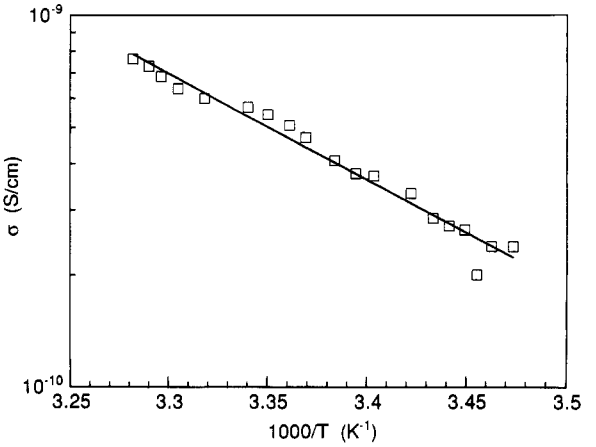

Figure 8. Variable temperature electrical conductivity data for a single crystal of $Cs_8Bi_4(P_2Se_6)_5$.

3.3. Electrical Conductivity Measurements. Four-probe electrical conductivity measurements on single crystals of $Cs_8Bi_4(P_2Se_6)_5$ showed that the material is a semiconductor with room temperature conductivity $\sigma \sim 10^{-9}$ S/cm, which drops to 10^{-10} S/cm at 253 K. Figure 8 shows the conductivity vs $1000/T$ semilog plot for $Cs_8Bi_4(P_2Se_6)_5$. The data can be fit to the equation shown below, suggesting a gap of $E_g = 1.135$ eV and an activation energy of $E_a = 0.567$ eV.

$$\sigma = \sigma_0 e^{-E_a/k_B T}$$

The value of 1.135 eV compares to 1.44 eV determined by optical spectroscopy (vide supra). The reason for the discrepancy is not known but may be due to the fact that the electrical conductivity does not represent the intrinsic semiconducting regime but may arise from impurity levels in the gap. It must be noted that the optical measurement

(32) Wacker, K.; Salk, M.; Decker-Schultheiss, G.; Kelley, E. *Z. Anorg. Allg. Chem.* **1991**, *606*, 51–58.
(33) Vos, A.; Wiegenga, E. H. *Acta Crystallogr.* **1955**, *8*, 217–223.

is the most reliable E_g indicator.[34] The antimony compound is an insulator.

In conclusion, new quaternary selenophosphates can be accessed with molten A/P/Se salts and this provides a useful synthetic approach with broad scope. For example, the new family of $A_2MP_2Se_6$ (A = K, Rb, Cs; M = Mn, Fe) compounds has been synthesized in this way.[35] The advantage of $A_x[P_ySe_z]$ fluxes is that they provide reliably $[P_2Se_6]^{4-}$ units which other conventional aqueous or organic solvents have trouble stabilizing due to the high negative charge. Thus, solid state and coordination chemistry with $[P_2Se_6]^{4-}$ and metal centers becomes tractable based on the methodology highlighted in this paper. It would be interesting to see whether changes in the nominal stoichiometry of these fluxes can result in other $[P_xSe_y]^{n-}$ units as well.

(34) Smith, R. A. *Semiconductors*; 2nd ed.; Cambridge University Press: New York, , 1978.
(35) McCarthy, T. J.; Kanatzidis, M. G. Manuscript in preparation.

Acknowledgment. Financial support from the National Science Foundation, DMR-9202428, is gratefully acknowledged. The X-ray instrumention used in this work was purchased in part with funds from the National Science Foundation (CHE-8908088). This work made use of the SEM facilities of the Center for Electron Optics at Michigan State University.

Supplementary Material Available: Tables giving observed and calculated X-ray powder diffraction patterns, atom coordinates, bond lengths, bond angles, and anisotropic thermal parameters (17 pages); a listing of calculated and observed ($10F_o$/$10F_c$) structure factors (43 pages). Ordering information is given on any current masthead page.